

## Supplementary Information

### Parallel-stranded DNA: Enhancing duplex stability by the ‘G-clamp’ and a pyrrolo-dC derivative

**Xin Ming,<sup>1</sup> Ping Ding,<sup>1,2</sup> Peter Leonard,<sup>1</sup> Simone Budow<sup>1</sup> and Frank Seela<sup>1,2\*</sup>**

<sup>1</sup>Laboratory of Bioorganic Chemistry and Chemical Biology, Center for Nanotechnology, Heisenbergstrasse 11, 48149 Münster, Germany and <sup>2</sup>Laboratorium für Organische und Bioorganische Chemie, Institut für Chemie, Universität Osnabrück, Barbarastrasse 7, 49069 Osnabrück, Germany

Corresponding author:

Prof. Dr. Frank Seela

Phone: +49 (0)251-53406-500

Fax: +49 (0)251-53406-587

E-mail: [Frank.Seela@uni-osnabrueck.de](mailto:Frank.Seela@uni-osnabrueck.de)

Home page: [www.seela.net](http://www.seela.net)

## Table of Contents

<b>Table S1.</b>	$^1\text{H}$ - $^{13}\text{C}$ -coupling constants of compounds <b>6</b> , <b>13</b> and <b>15</b> .....	2
<b>Table S2.</b>	Molecular masses of oligonucleotides determined by mass spectrometry.....	3
<b>Figure S1.</b>	LC-ESI-MS chromatogram of ODN- <b>28</b> .....	4
<b>Figure S2.</b>	LC-ESI-MS chromatogram of ODN- <b>29</b> .....	5
<b>Figure S3.</b>	Maldi-TOF mass spectrum of ODN- <b>33</b> .....	6
<b>Figure S4.</b>	Maldi-TOF mass spectrum of ODN- <b>34</b> .....	7
<b>Figure S5.</b>	Maldi-TOF mass spectrum of ODN- <b>35</b> .....	8
<b>Figure S6.</b>	Melting curves of parallel stranded duplexes <b>27•30</b> , <b>28•30</b> , <b>29•30</b> , <b>28•31</b> . ....	9
<b>Figure S7.</b>	Melting curves of parallel stranded duplexes <b>24•26</b> , <b>32•33</b> , <b>34•33</b> , <b>35•33</b> , <b>32•36</b> , <b>34•36</b> and <b>35•36</b> .....	10-11
<b>Figure S8.</b>	Melting curves of antiparallel stranded duplexes <b>24•25</b> , <b>32•37</b> , <b>34•37</b> and <b>35•37</b> .....	12
<b>Figure S9.</b>	$^1\text{H}$ -NMR spectrum of compound <b>6</b> .....	13
<b>Figure S10.</b>	$^{13}\text{C}$ -NMR spectrum of compound <b>6</b> .....	14
<b>Figure S11.</b>	DEPT-135 spectrum of compound <b>6</b> .....	15
<b>Figure S12.</b>	$^1\text{H}$ - $^{13}\text{C}$ -gated decoupled spectrum of compound <b>6</b> .....	16
<b>Figure S13.</b>	$^1\text{H}$ -NMR spectrum of compound <b>13</b> .....	17
<b>Figure S14.</b>	$^{13}\text{C}$ -NMR spectrum of compound <b>13</b> .....	18
<b>Figure S15.</b>	DEPT-135 spectrum of compound <b>13</b> .....	19
<b>Figure S16.</b>	$^1\text{H}$ - $^{13}\text{C}$ -gated decoupled spectrum of compound <b>13</b> .....	20
<b>Figure S17.</b>	$^1\text{H}$ -NMR spectrum of compound <b>15</b> .....	21
<b>Figure S18.</b>	$^{13}\text{C}$ -NMR spectrum of compound <b>15</b> .....	22
<b>Figure S19.</b>	DEPT-135 spectrum of compound <b>15</b> .....	23
<b>Figure S20.</b>	$^1\text{H}$ - $^{13}\text{C}$ -gated decoupled spectrum of compound <b>15</b> .....	24
<b>Figure S21.</b>	$^{31}\text{P}$ -NMR spectrum of compound <b>5</b> .....	25
<b>Figure S22.</b>	$^1\text{H}$ -NMR spectrum of the DMT-protected G-clamp.....	26
<b>Figure S23.</b>	$^{13}\text{C}$ -NMR spectrum of the DMT-protected G-clamp .....	27
<b>Figure S24.</b>	$^1\text{H}$ -NMR spectrum of compound <b>16</b> .....	28
<b>Figure S25.</b>	$^{13}\text{C}$ -NMR spectrum of compound <b>16</b> .....	29
<b>Figure S26.</b>	$^{31}\text{P}$ -NMR spectrum of compound <b>16</b> .....	30

**Table S1.**  $^1\text{H}$ - $^{13}\text{C}$ -coupling constants of compounds **6**, **13** and **15**.<sup>a,b</sup>

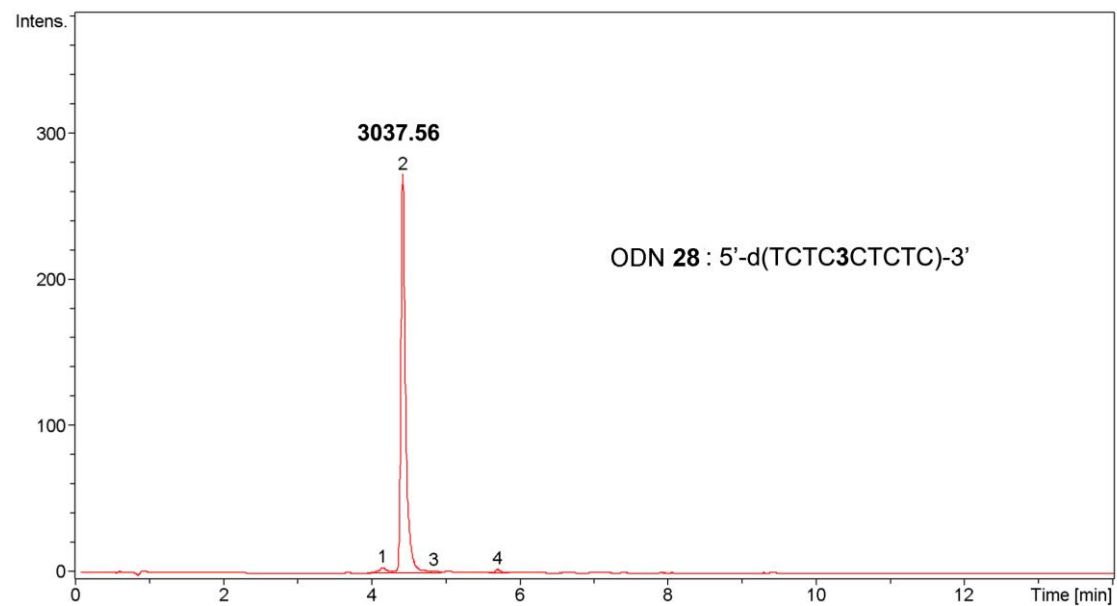
$^1\text{H}$ - $^{13}\text{C}$ coupling constants	$J$ [Hz]		
	<b>6</b>	<b>13</b>	<b>15</b>
$^1J(\text{C4}, \text{H-C4})$	187.4	-	182.6
$^2J(\text{C4a}, \text{H-C4})$	3.6	-	-
$^3J(\text{C7a}, \text{H-C4})$	7.1	-	7.5
$^1J(\text{C5}, \text{H-C5})$	185.4	-	178.8
$^2J(\text{C4a}, \text{H-C5})$	3.6	-	-
$^3J(\text{C7a}, \text{H-C5})$	7.1	-	7.5
$^2J(\text{C6}, \text{H-C5})$	5.0	-	9.8
$^1J(\text{C1}', \text{H-C1}')$	173.5	-	174.6
$^1J(\text{C3}', \text{H-C3}')$	147.3	-	148.1
$^1J(\text{C4}', \text{H-C4}')$	146.3	-	146.3
$^1J(\text{C5}', \text{H-C5}')$	139.4	-	141.3
$^1J(\text{C1}'', \text{H-C1}'')$	-	142.1	142.1
$^1J(\text{C2}'', \text{H-C2}'')$	-	129.8	130.1
$^1J(\text{C3}'', \text{H-C3}'')$	-	139.1	139.3

<sup>a</sup> Measured in  $\text{DMSO-}d_6$  at 298 K. <sup>b</sup> Systematic numbering.

**Table S2.** Molecular masses of oligonucleotides determined by mass spectrometry.

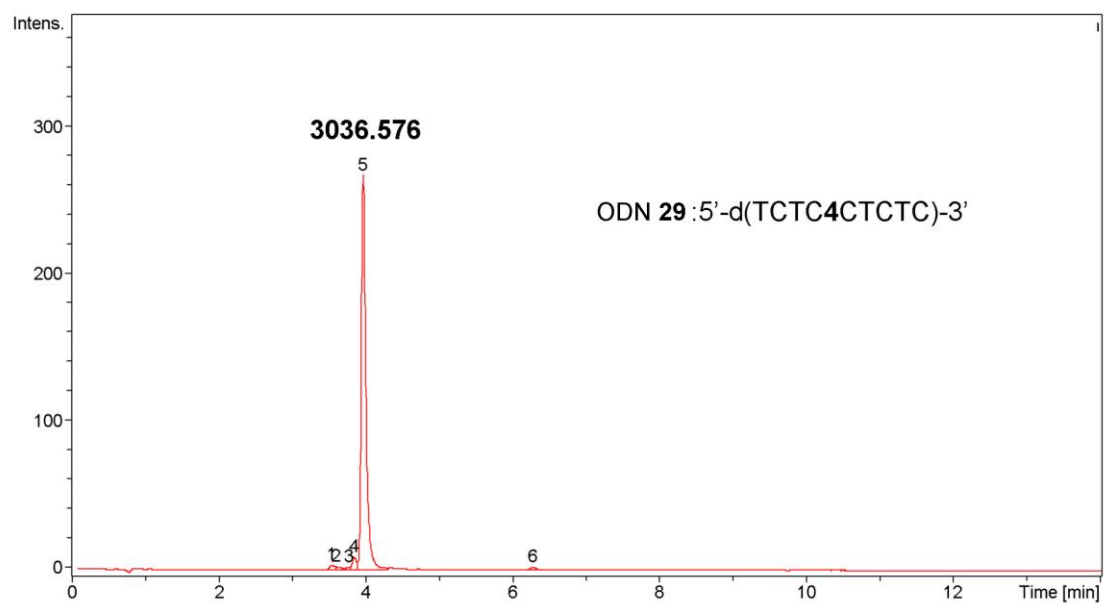
	Sequence	Mol. Wt. (calc.)	Mol. Wt. (found)
ODN-28	5'-d(TCTC3CTCTC)-3'	3038	3038 <sup>a</sup>
ODN-29	5'-d(TCTC4CTCTC)-3'	3037	3037 <sup>a</sup>
ODN-33	5'-d(TT1 TTT TTT TAT TAA AAT TTA T1A A)-3'	7665	7664 <sup>b</sup>
ODN-34	5'-d(AA3 AAA AAA ATA ATT TTA AAT A3T T)-3'	7945	7948 <sup>c</sup>
ODN-35	5'-d(AA4 AAA AAA ATA ATT TTA AAT A4T T)-3'	7944	7944 <sup>c</sup>

<sup>a</sup> Measured by LC-ESI-TOF mass spectrometry. <sup>b</sup> Measured by MALDI-TOF mass spectrometry in the linear negative mode. <sup>c</sup> Measured by MALDI-TOF mass spectrometry in the linear positive mode.



#	RT [min]	Area Frac. %	Max. MW
1	4.2	2.3	3070.532
2	4.4	96.0	3037.561
3	4.8	0.7	3037.525
4	5.7	1.0	4729.804

**Figure S1.** LC-ESI-MS chromatogram of ODN-28.



#	RT [min]	Area Frac. %	Max. MW
1	3.5	1.2	2732.490
2	3.6	0.9	2747.488
3	3.8	0.6	
4	3.8	2.8	3036.556
5	4.0	93.7	3036.576
6	6.3	0.8	

**Figure S2.** LC-ESI-MS chromatogram of ODN-29.

**Applied Biosystems Voyager System 6327**

Voyager Spec #1=>MC[BP = 8453.2, 2972]

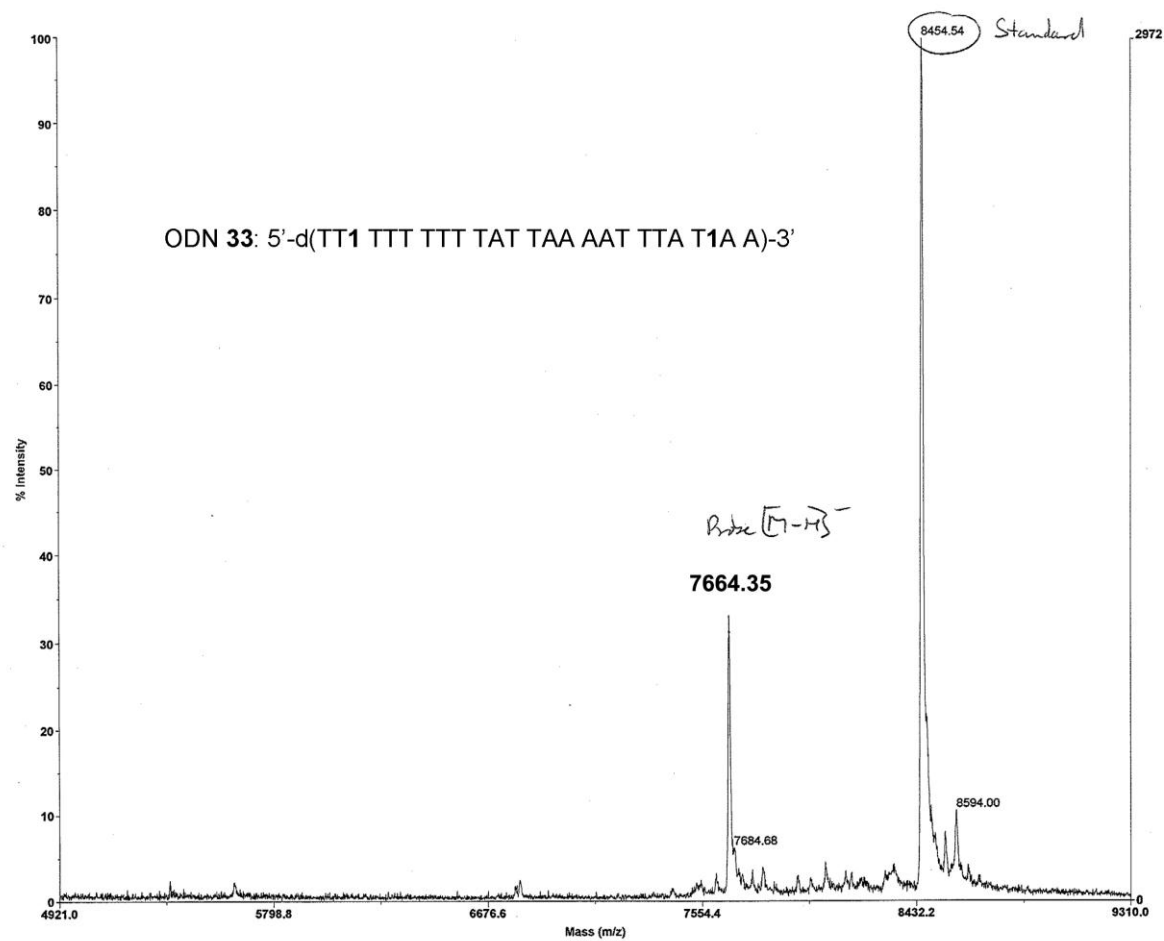


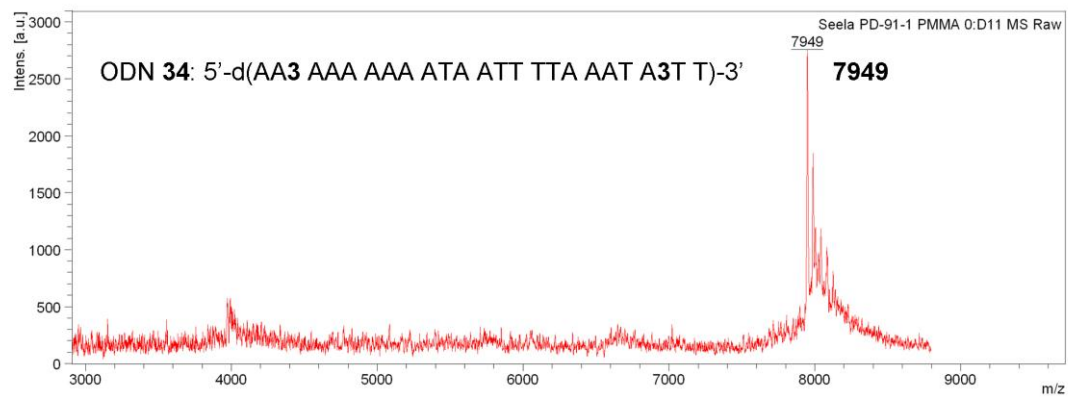
**Figure S3.** Maldi-TOF mass spectrum of ODN-33.

---

Bruker Autoflex Speed

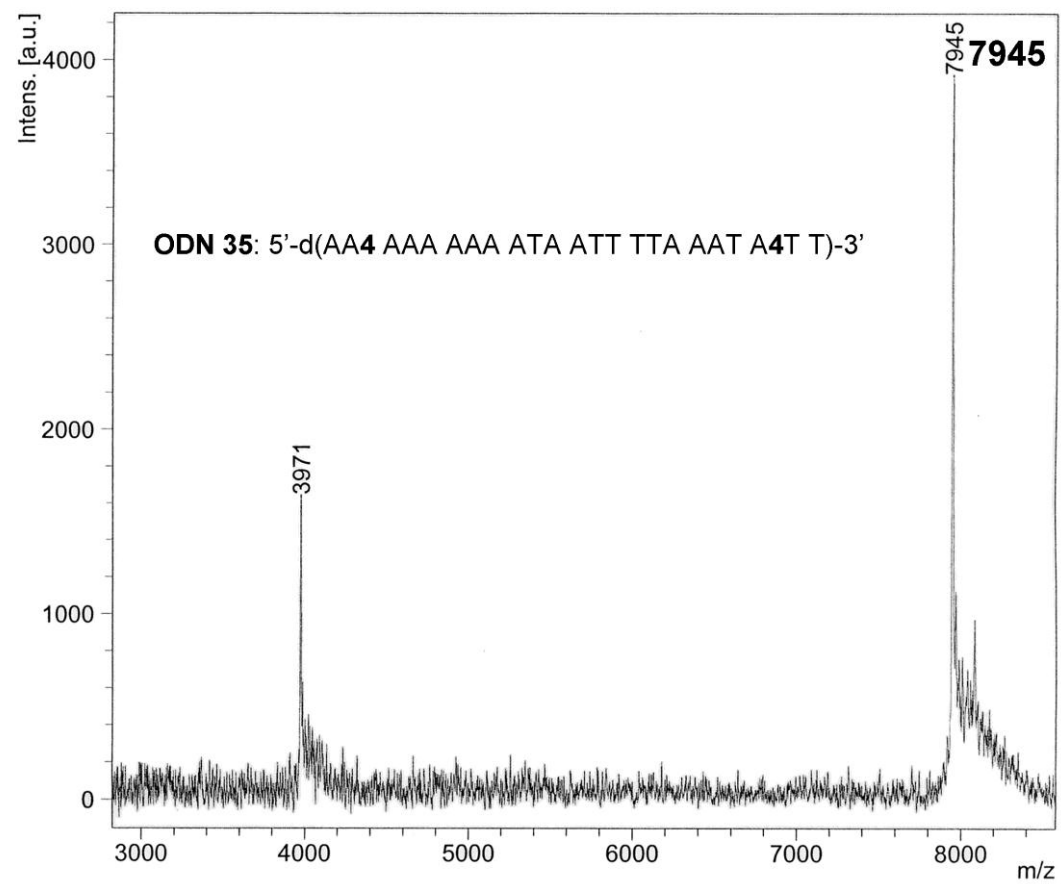
Org. Chem. Inst. WWU

---

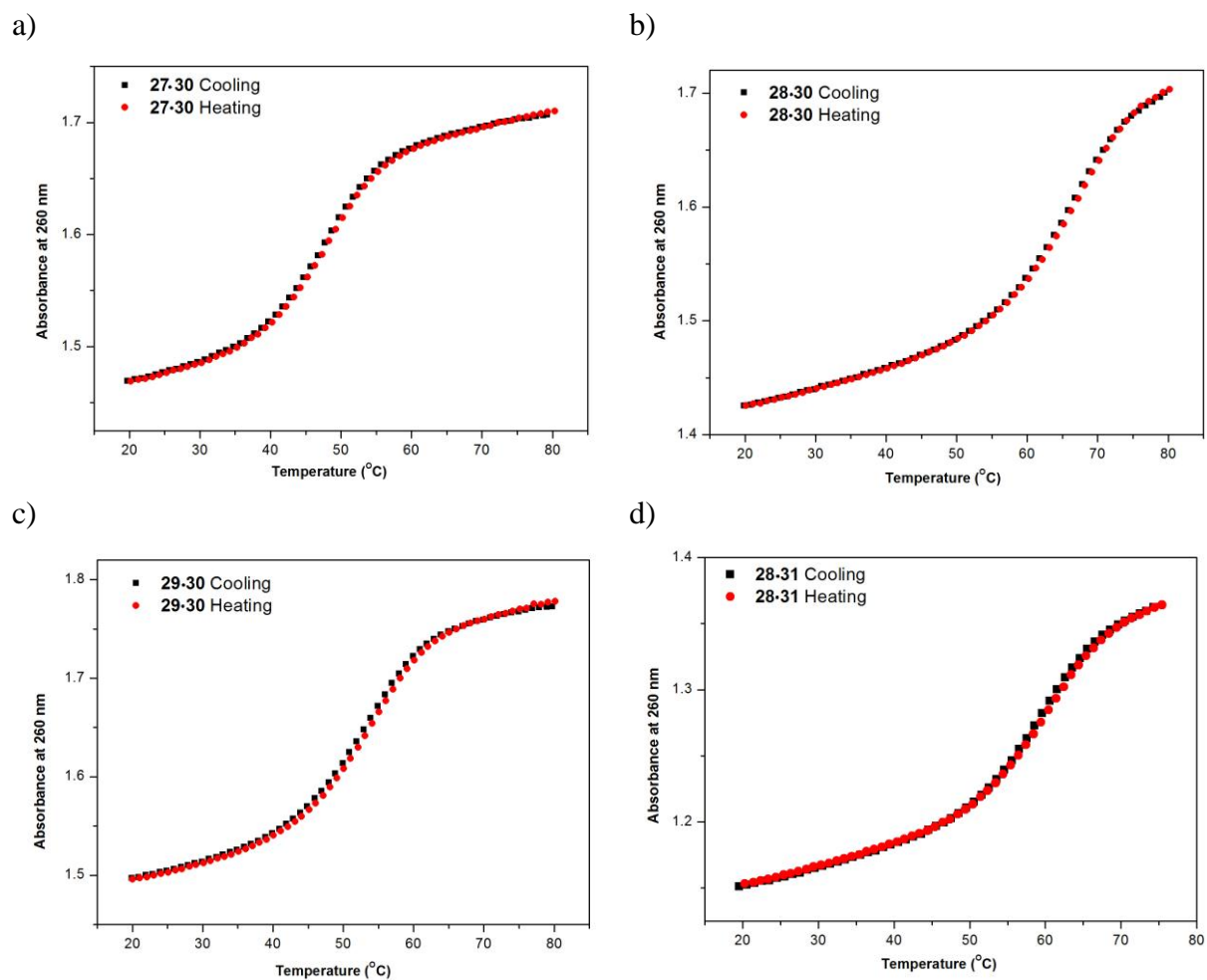


**Figure S4.** Maldi-TOF mass spectrum of ODN-34.

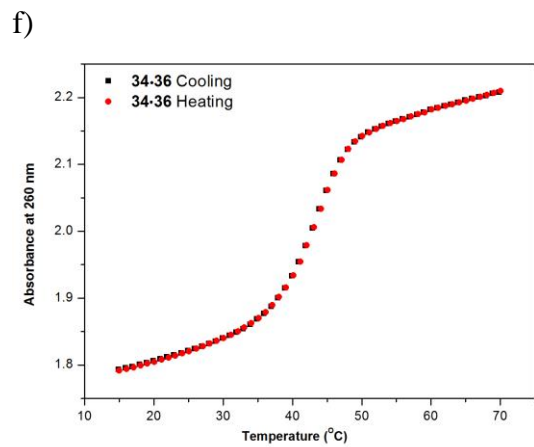
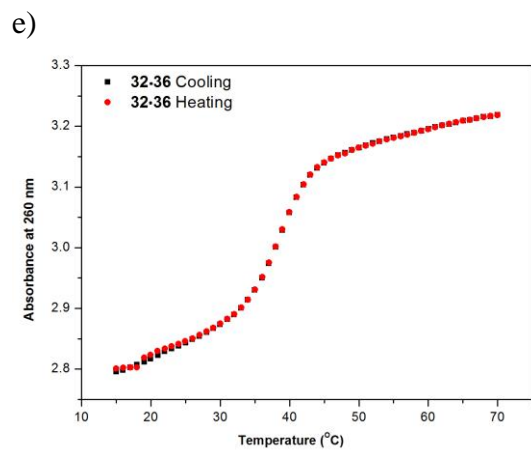
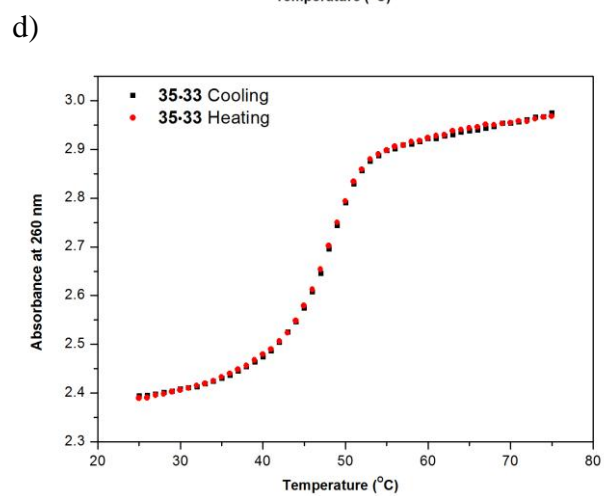
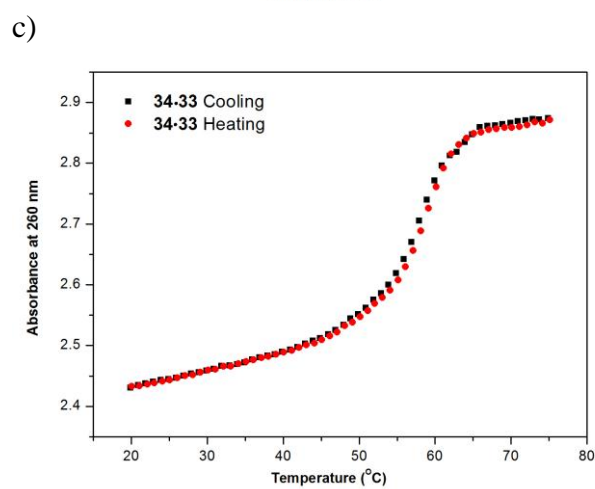
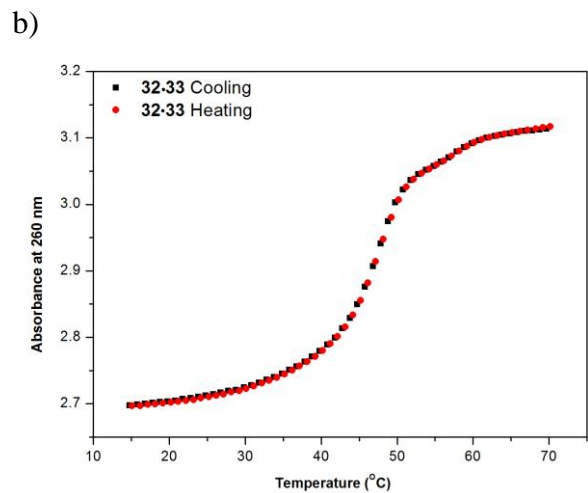
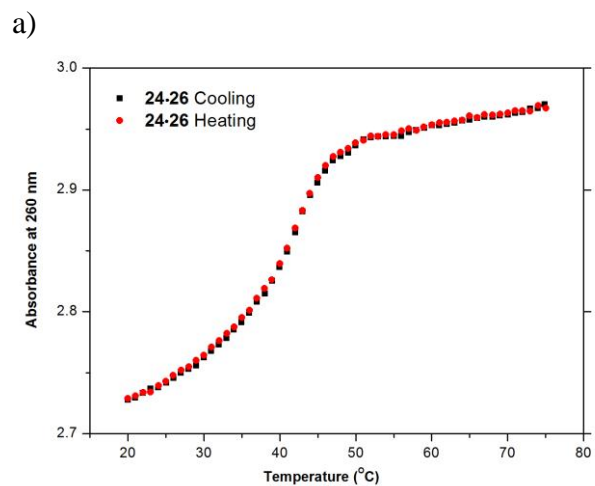




**Figure S5.** Maldi-TOF mass spectrum of ODN-35.



**Figure S6.** Melting curves of parallel stranded duplexes obtained from cooling (black square) and heating (red circle) experiments monitored at 260 nm and measured in 0.1 M NaCl, 10 mM MgCl<sub>2</sub>, 10 mM Na-cacodylate (pH 7.0) with 5 μM + 5 μM single-strand concentration. (a) Duplex **27•30**; (b) duplex **28•30**; (c) duplex **29•30** and (d) duplex **28•31**.



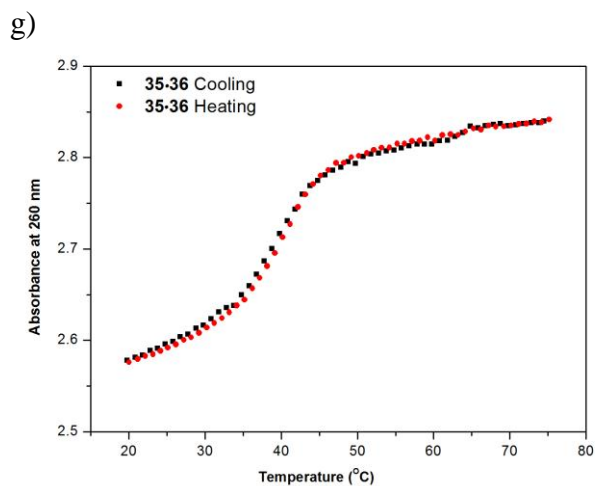


**Figure S7.** Melting curves of parallel stranded duplexes obtained from cooling (black square) and heating (red circle) experiments monitored at 260 nm and measured in 0.1 M NaCl, 10 mM MgCl<sub>2</sub>, 10 mM Na-cacodylate (pH 7.0) with 5 μM + 5 μM single-strand concentration. (a) Duplex **24•26**; (b) duplex **32•33**; (c) duplex **34•33**; (d) duplex **35•33**; (e) duplex **32•36**; (f) duplex **34•36** and (g) duplex **35•36**.

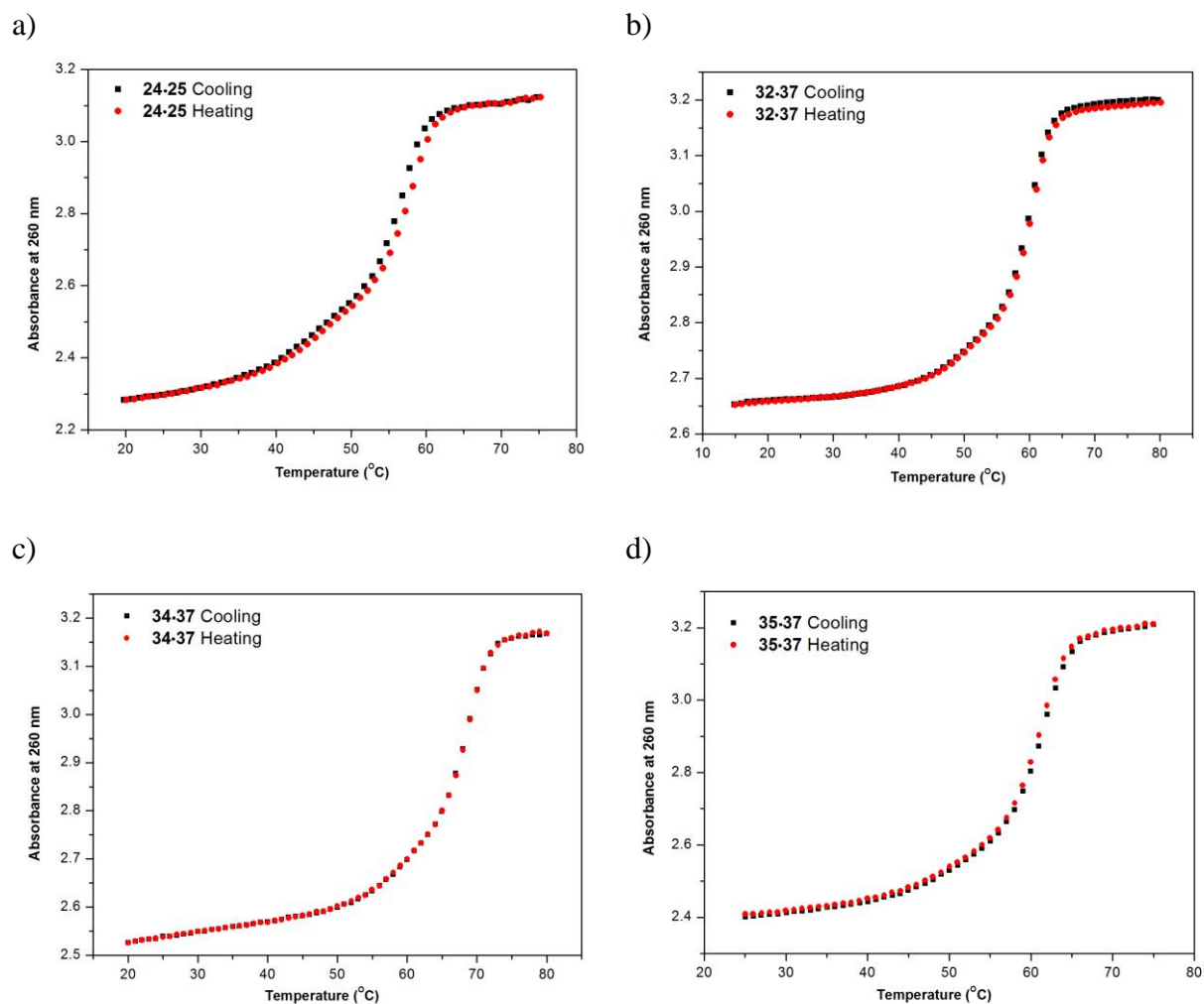


**Figure S8.** Melting curves of antiparallel stranded duplexes obtained from cooling (black square) and heating (red circle) experiments monitored at 260 nm and measured in 0.1 M NaCl, 10 mM MgCl<sub>2</sub>, 10 mM Na-cacodylate (pH 7.0) with 5 μM + 5 μM single-strand concentration. (a) Duplex **24•25**; (b) duplex **32•37**; (c) duplex **34•37** and (d) duplex **35•37**.

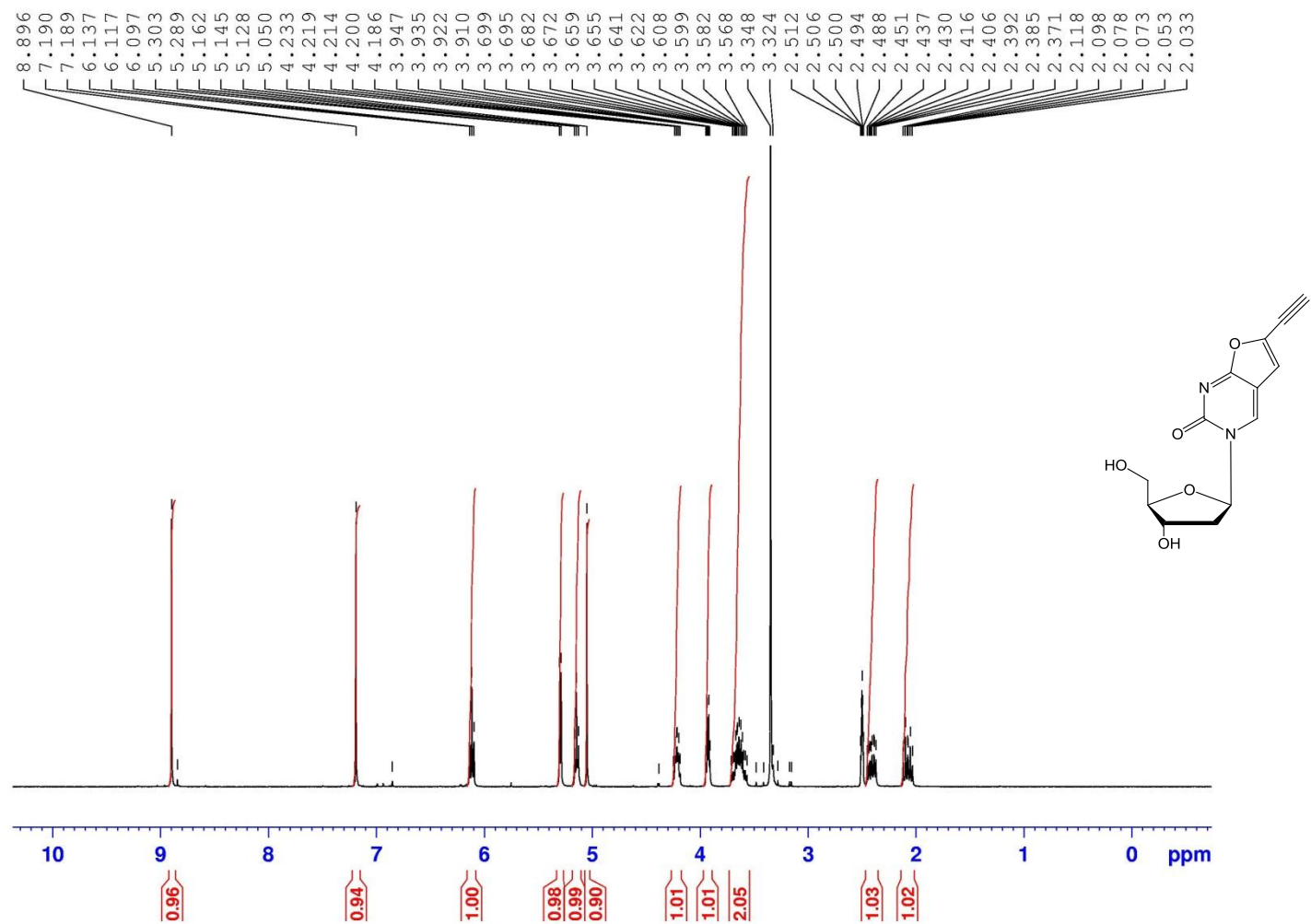


**Figure S9.** <sup>1</sup>H-NMR spectrum of 3-(2-deoxy-β-D-erythro-pentofuranosyl)-6-ethynyl-furo[2,3-d]pyrimidin-2(3H)-one (**6**).

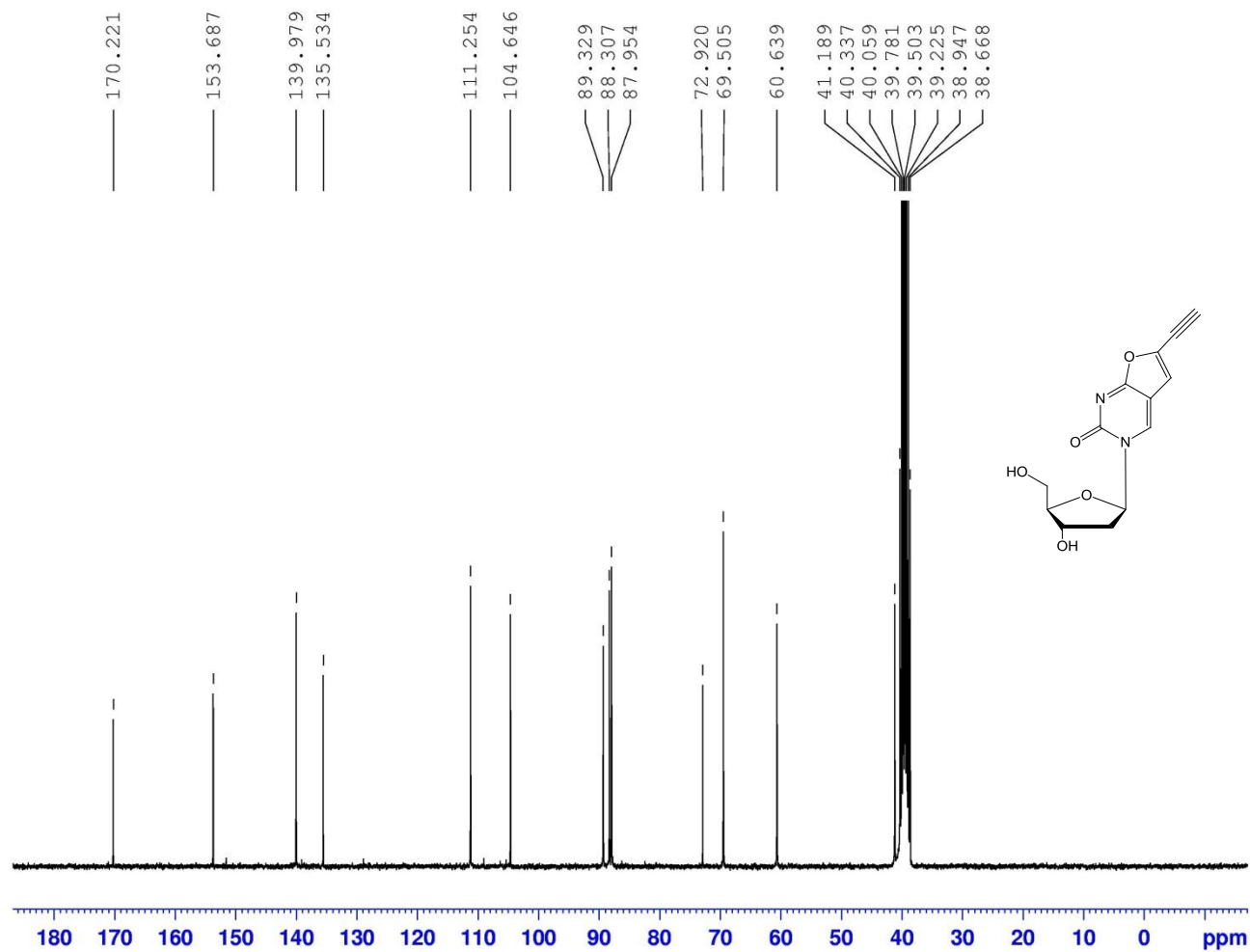


**Figure S10.** <sup>13</sup>C-NMR spectrum of 3-(2-deoxy-β-D-erythro-pentofuranosyl)-6-ethynyl-furo[2,3-d]pyrimidin-2(3H)-one (**6**).

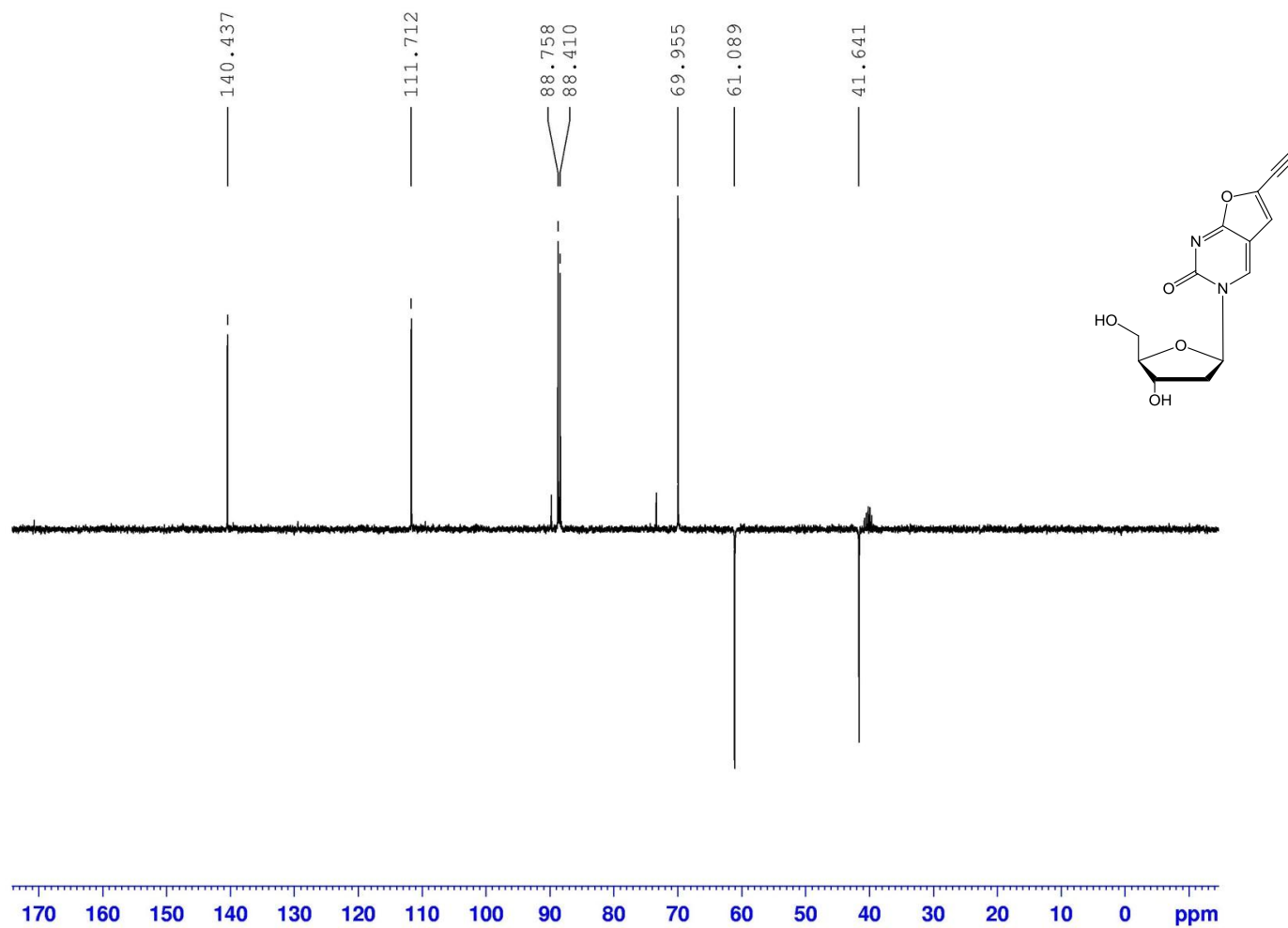


**Figure S11.** DEPT-135 spectrum of 3-(2-deoxy-β-D-erythro-pentofuranosyl)-6-ethynyl-furo[2,3-d]pyrimidin-2(3H)-one (**6**).



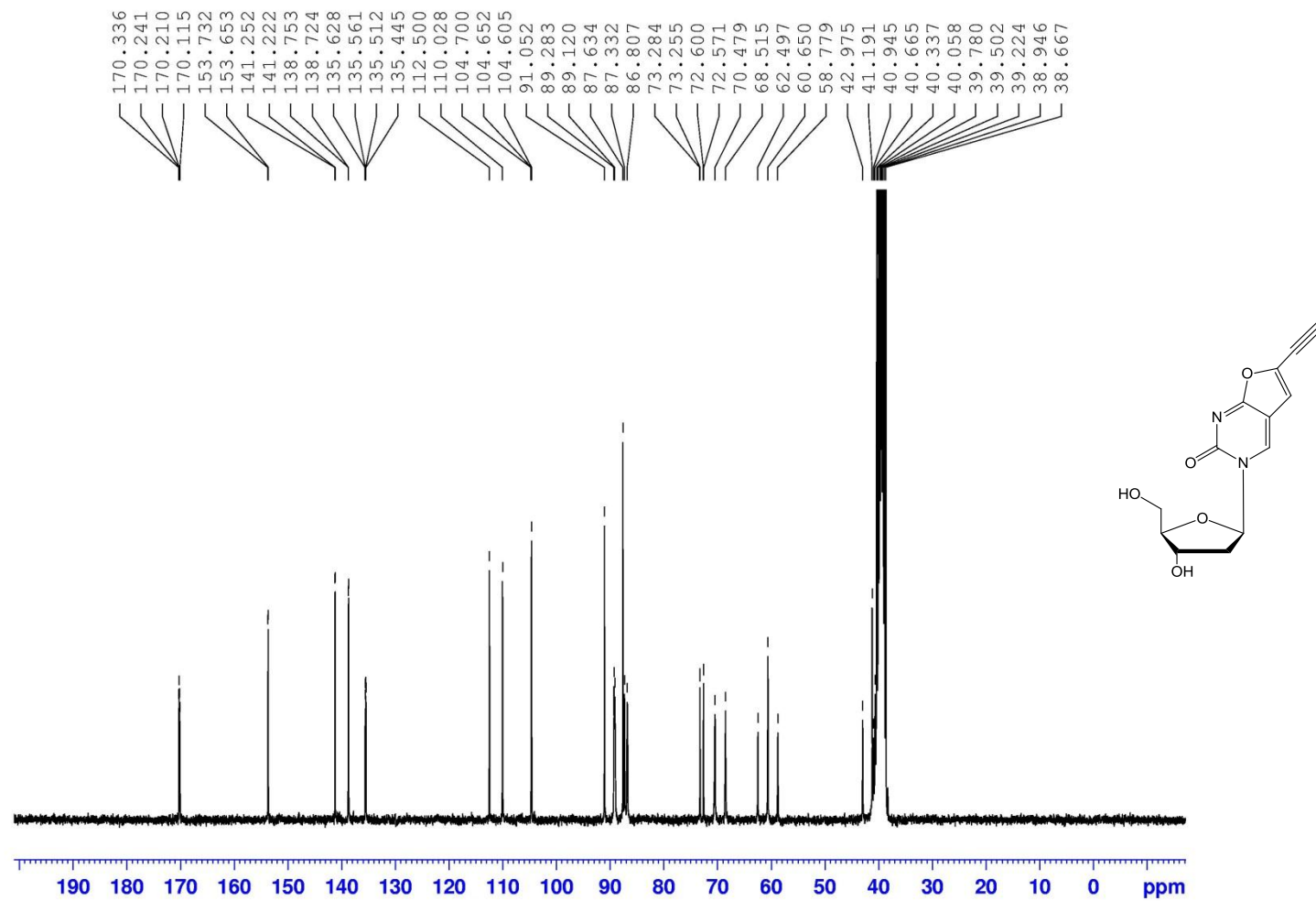


**Figure S12.**  $^1\text{H}$ - $^{13}\text{C}$ -gated decoupled spectrum of 3-(2-deoxy- $\beta$ -D-erythro-pentofuranosyl)-6-ethynyl-furo[2,3-*d*]pyrimidin-2(3*H*)-one (**6**).

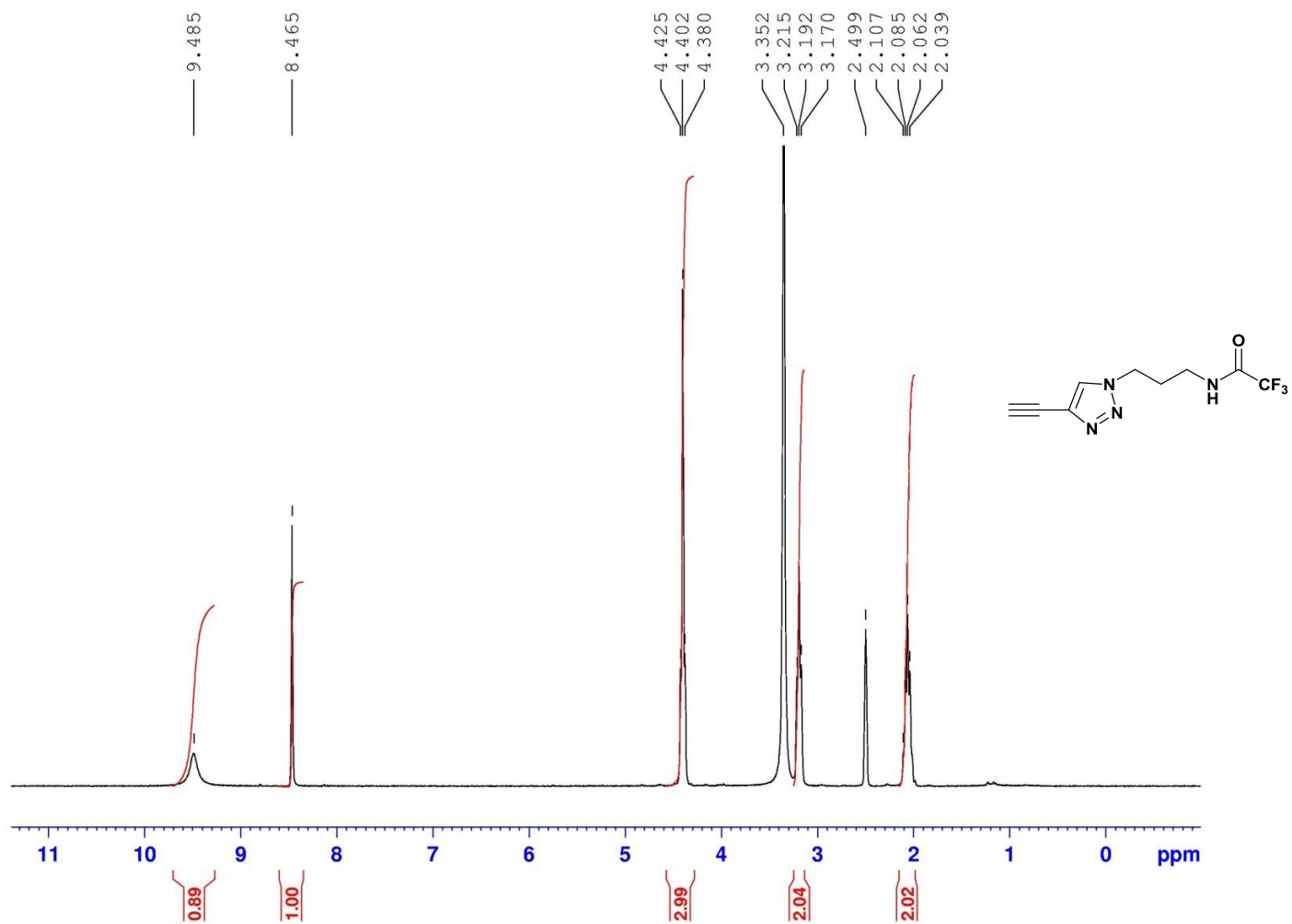


**Figure S13.** <sup>1</sup>H-NMR spectrum of *N*-(3-(4-ethynyl-1*H*-1,2,3-triazol-1-yl)propyl)-2,2,2-trifluoroacetamide (**13**).

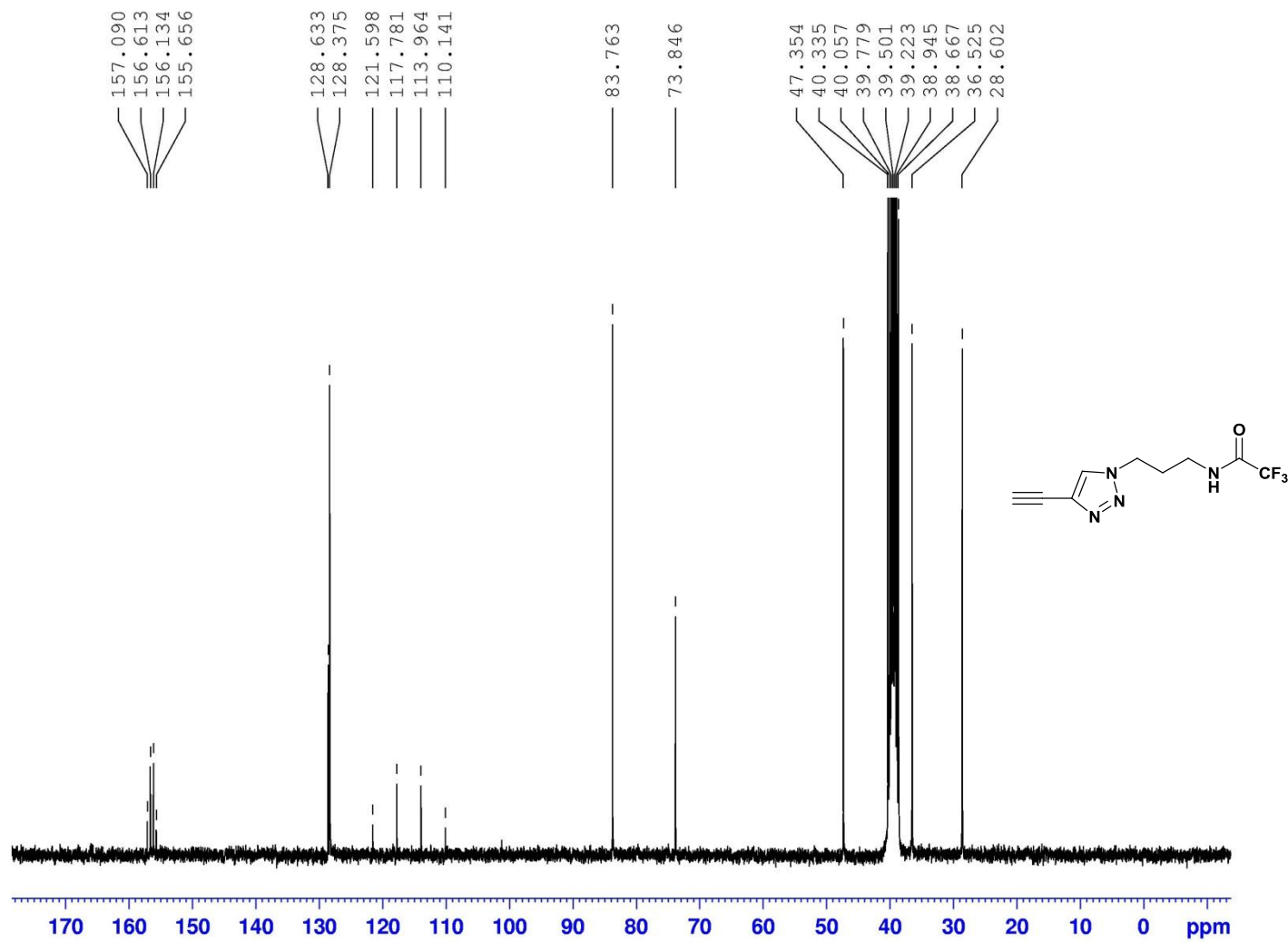


**Figure S14.**  $^{13}\text{C}$ -NMR spectrum of *N*-(3-(4-ethynyl-1*H*-1,2,3-triazol-1-yl)propyl)-2,2,2-trifluoroacetamide (13).

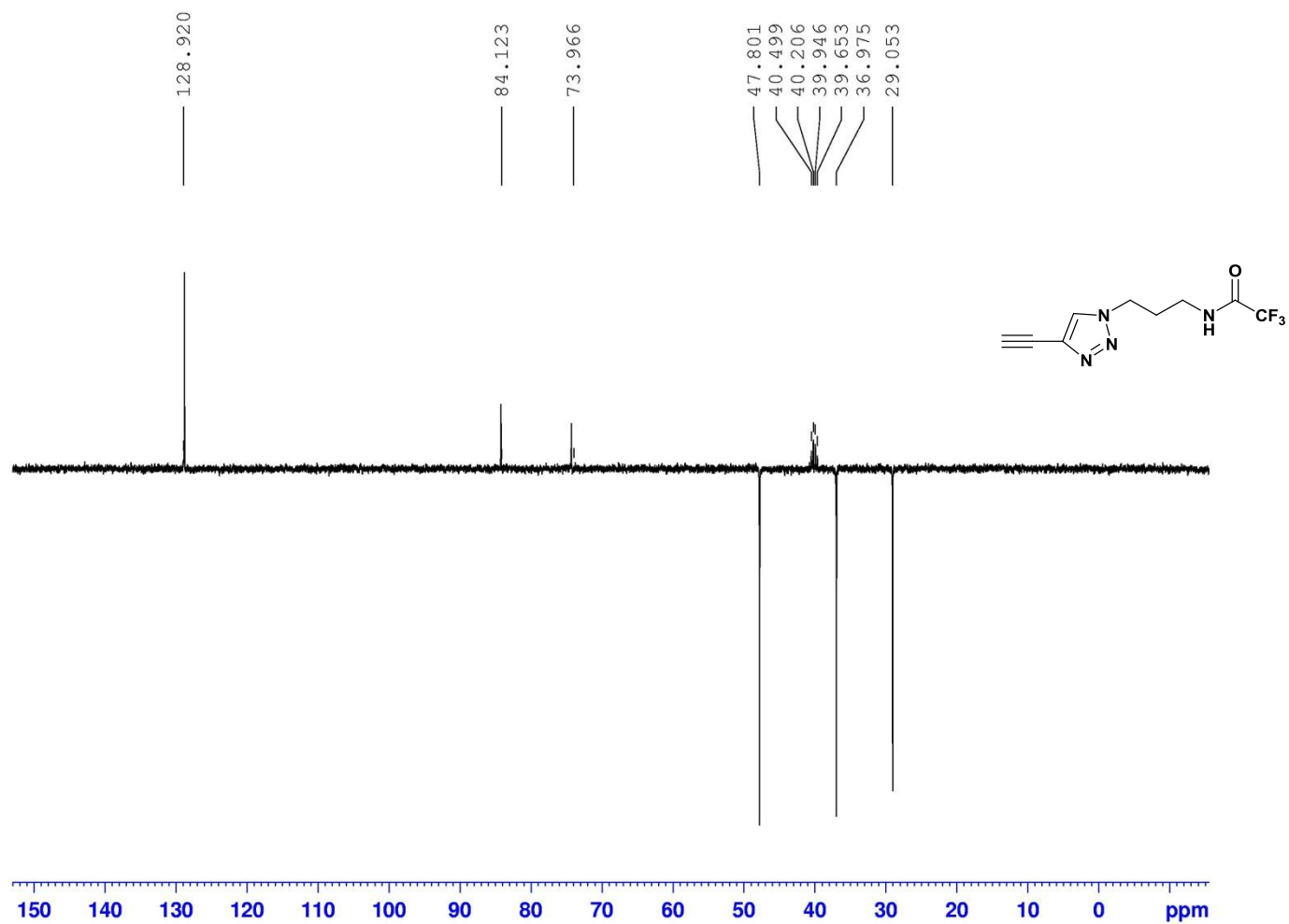


**Figure S15.** DEPT-135 spectrum of *N*-(3-(4-ethynyl-1*H*-1,2,3-triazol-1-yl)propyl)-2,2,2-trifluoroacetamide (**13**).

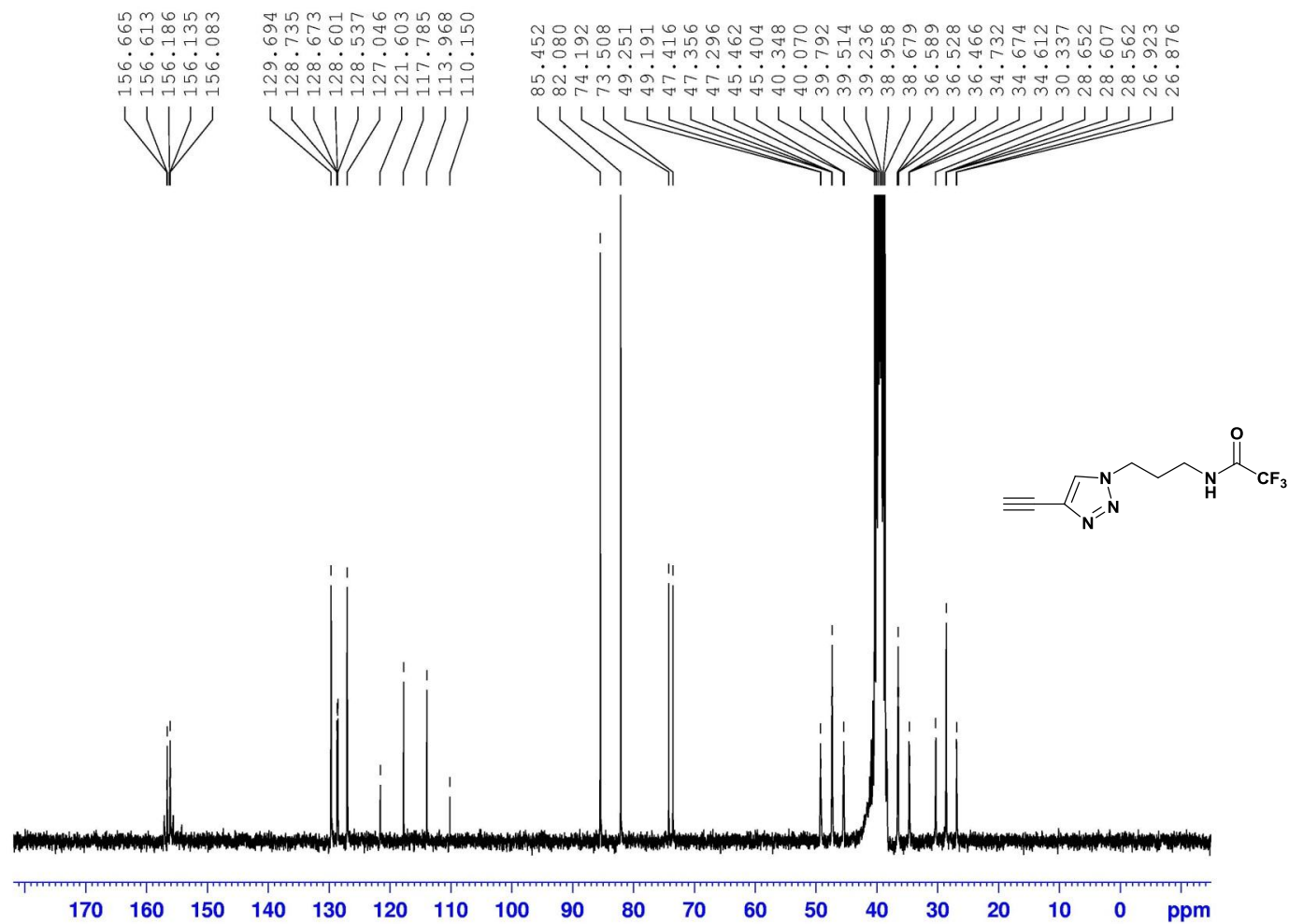


**Figure S16.**  $^1\text{H}$ - $^{13}\text{C}$ -gated decoupled spectrum of *N*-(3-(4-ethynyl-1*H*-1,2,3-triazol-1-yl)propyl)-2,2,2-trifluoroacetamide (**13**).

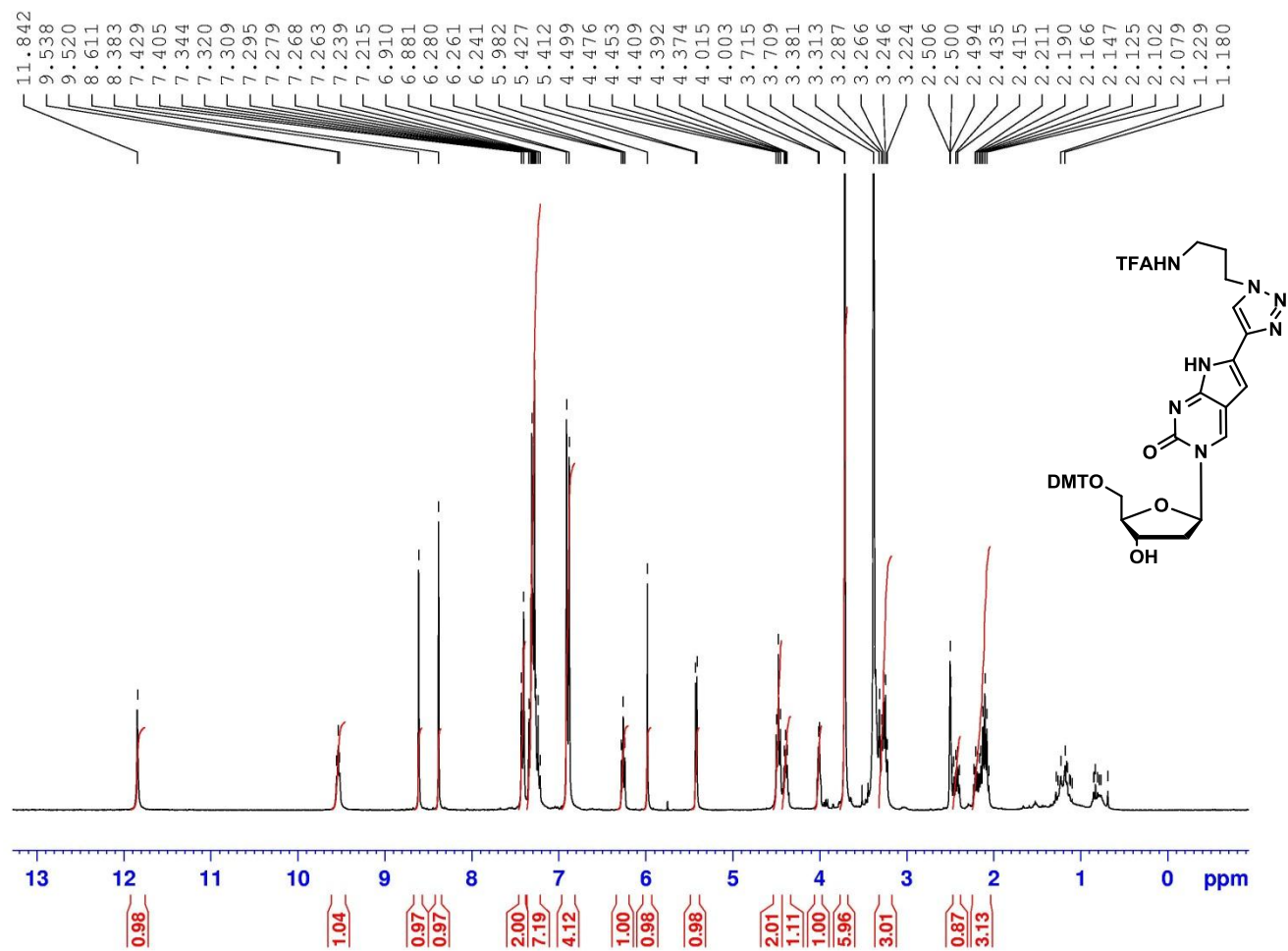


**Figure S17.** <sup>1</sup>H-NMR spectrum of trifluoroacetamide protected pyrrolo-dC analogue with DMT (**15**).

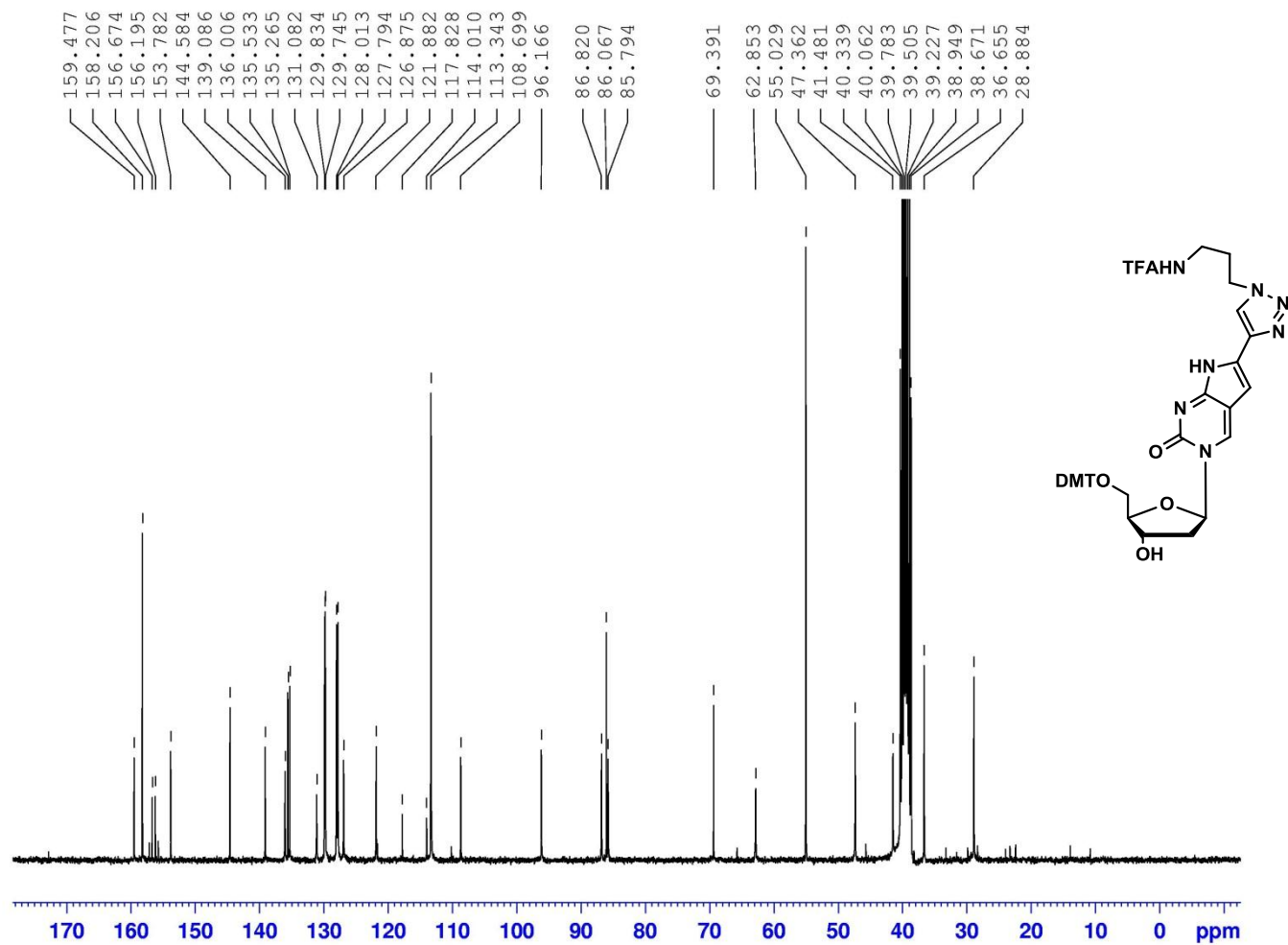


**Figure S18.**  $^{13}\text{C}$ -NMR spectrum of trifluoroacetamide protected pyrrolo-dC analogue with DMT (**15**).

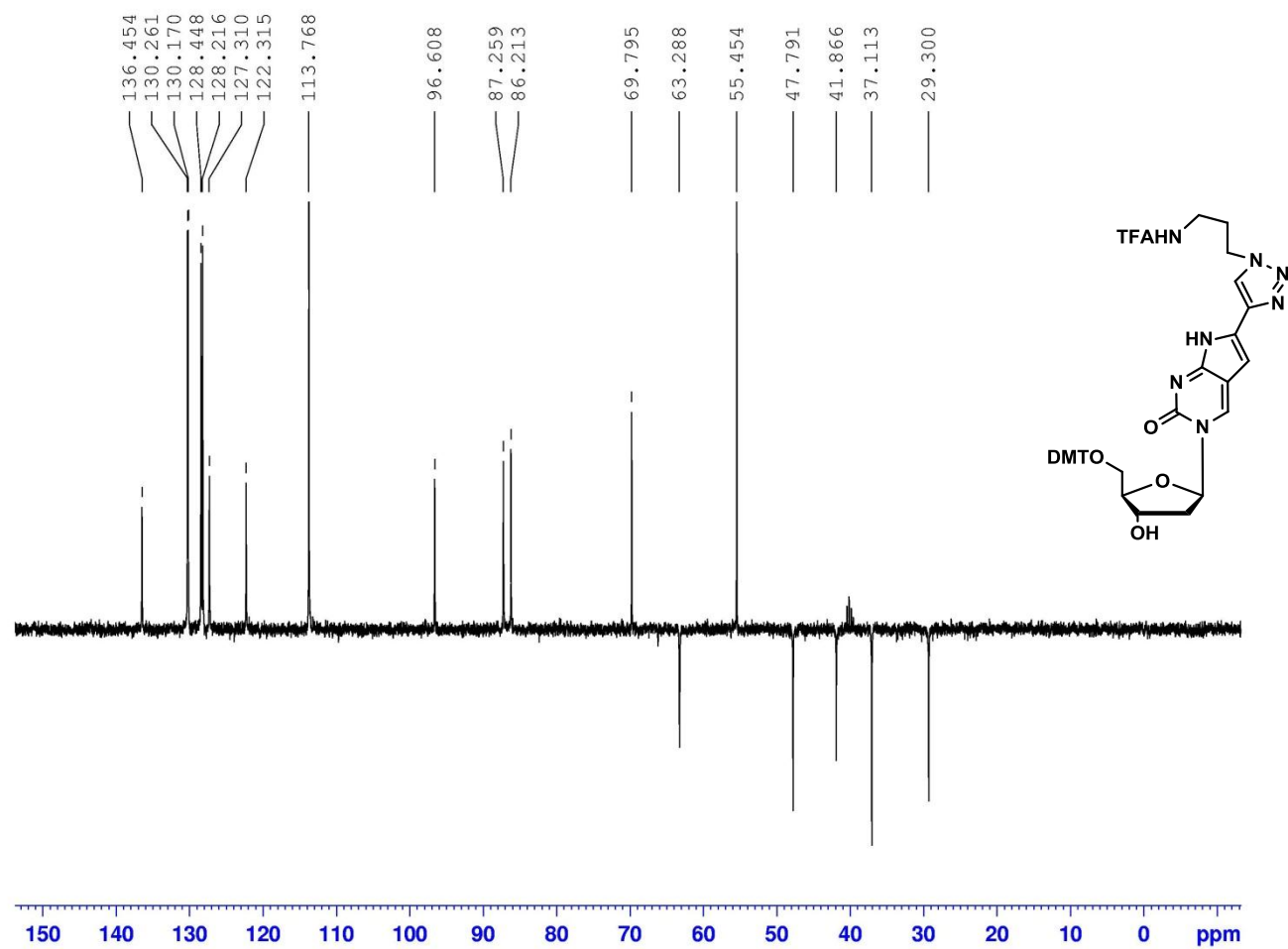


**Figure S19.** DEPT-135 spectrum of trifluoroacetamide protected pyrrolo-dC analogue with DMT (**15**).



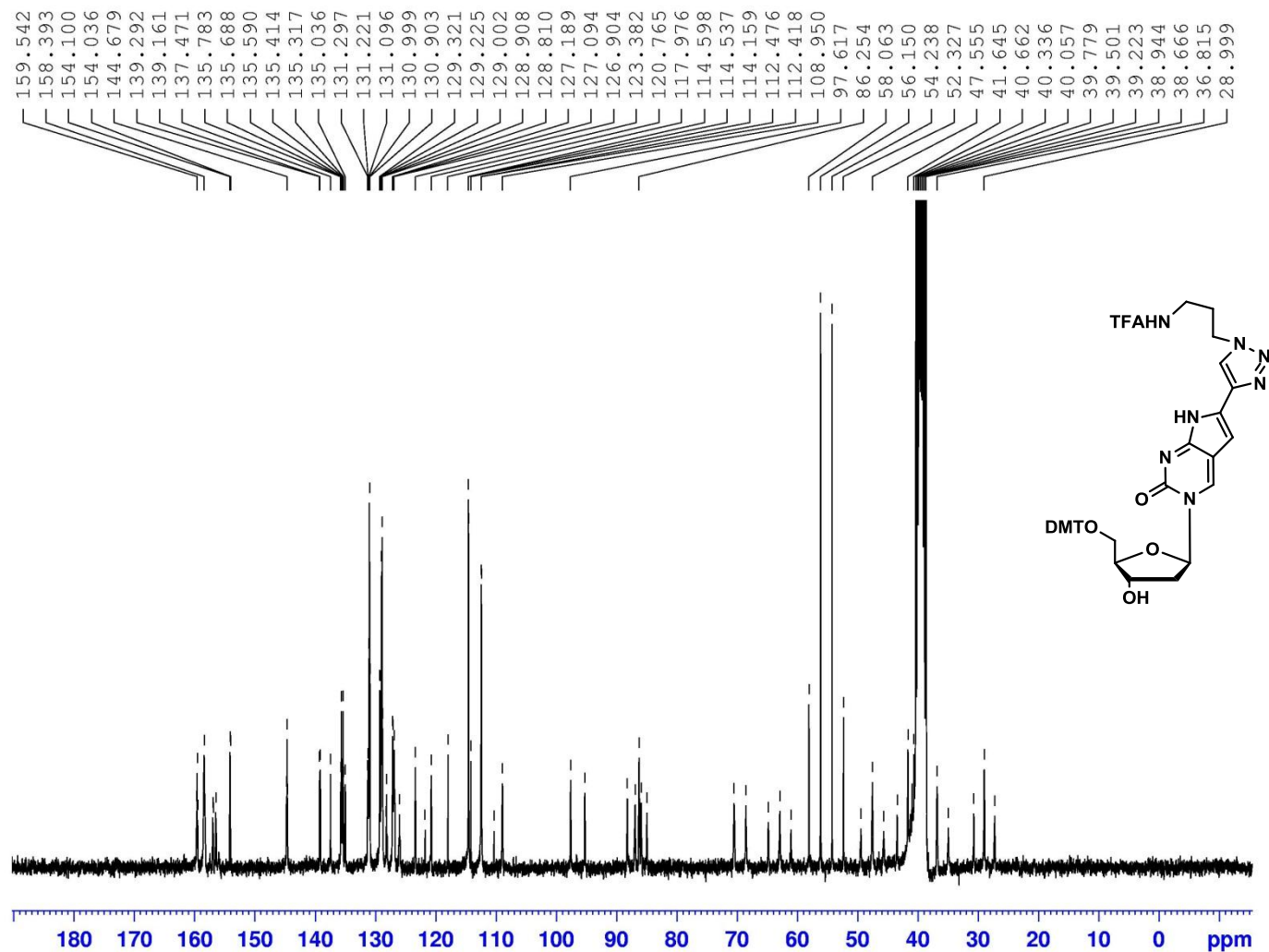


**Figure S20.**  $^1\text{H}$ - $^{13}\text{C}$ -gated decoupled spectrum of trifluoroacetamide protected pyrrolo-dC analogue with DMT (**15**).

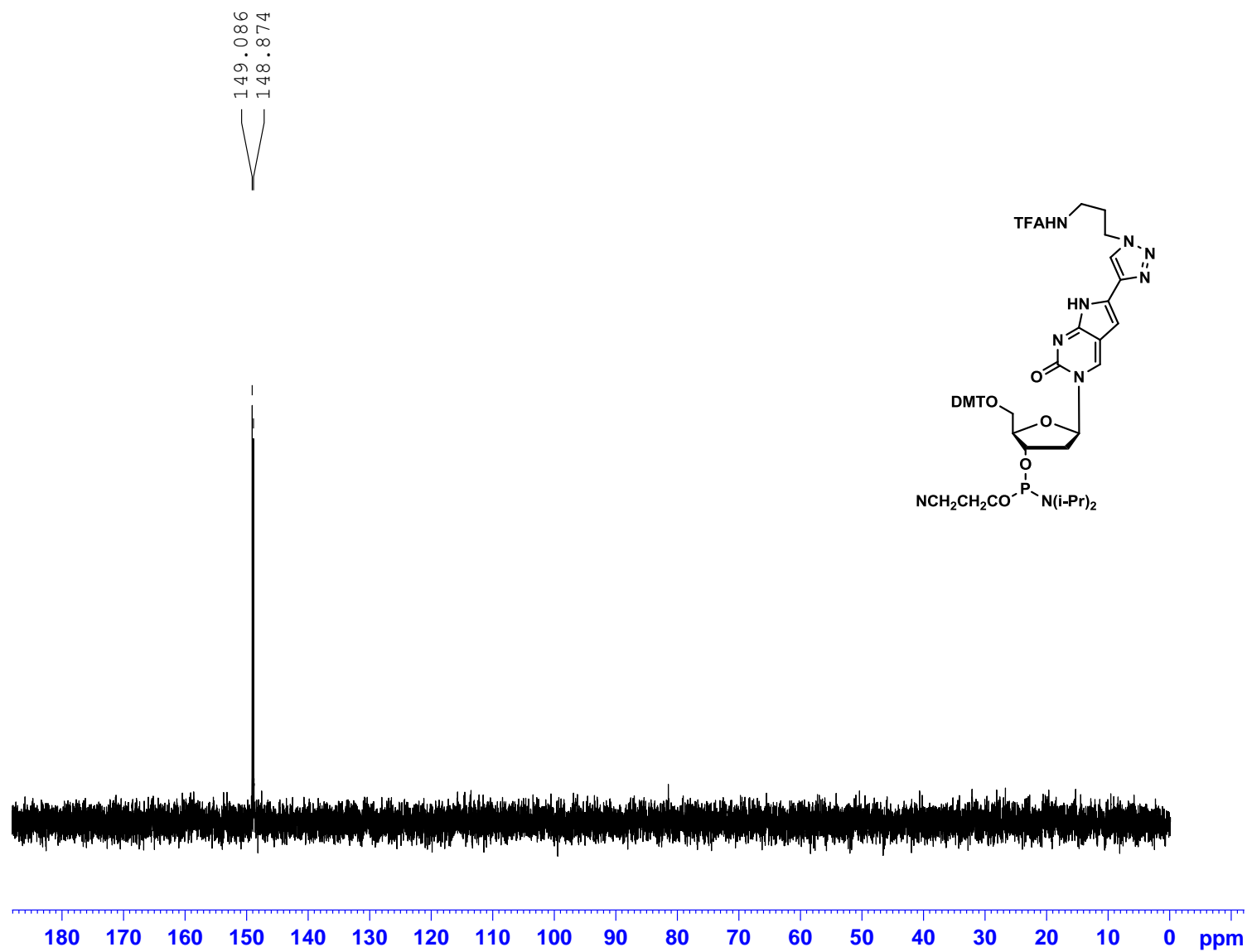


Figure S21.  $^{31}\text{P}$ -NMR spectrum of phosphoramidite 5.

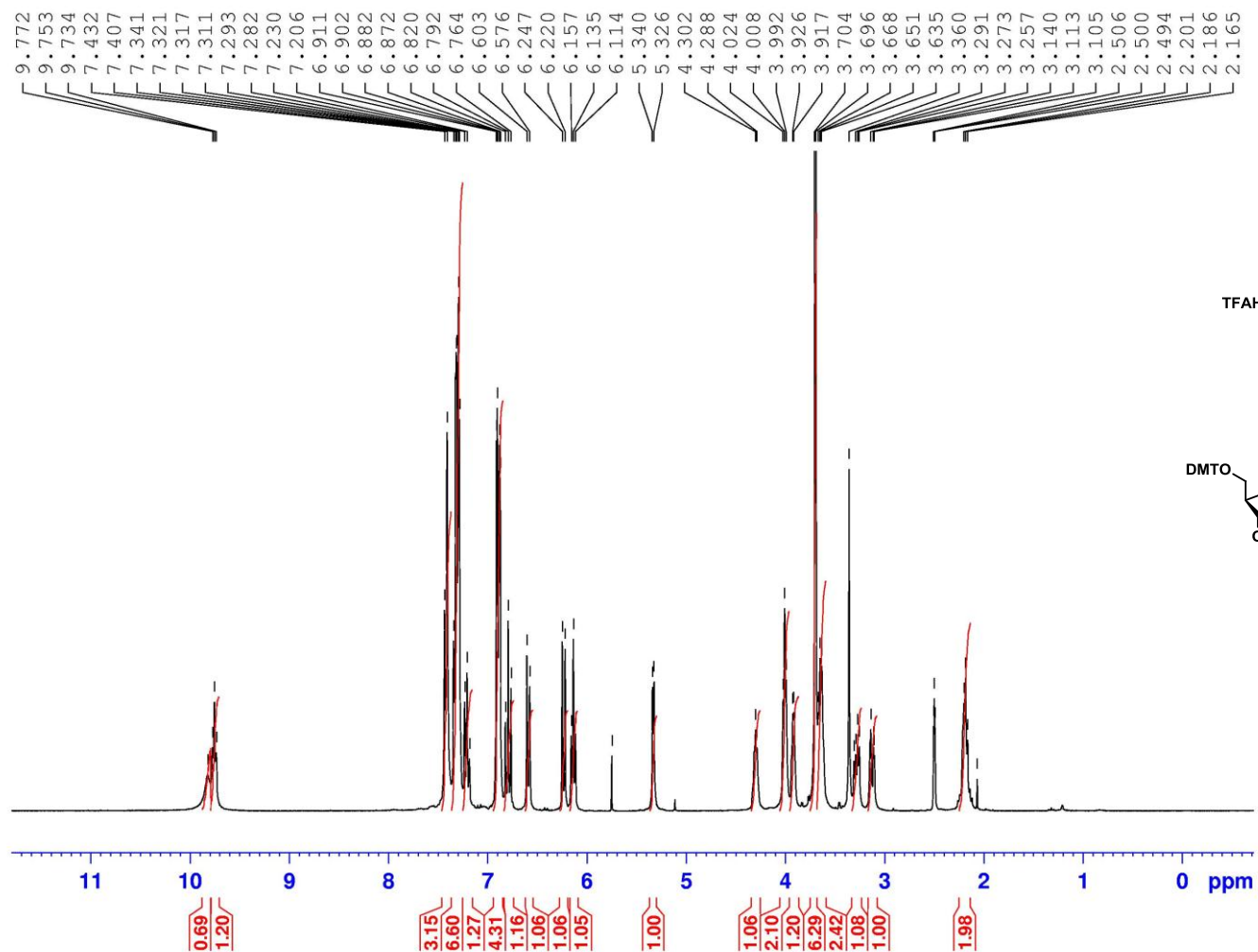


Figure S22. <sup>1</sup>H-NMR spectrum of the DMT-protected G-clamp.

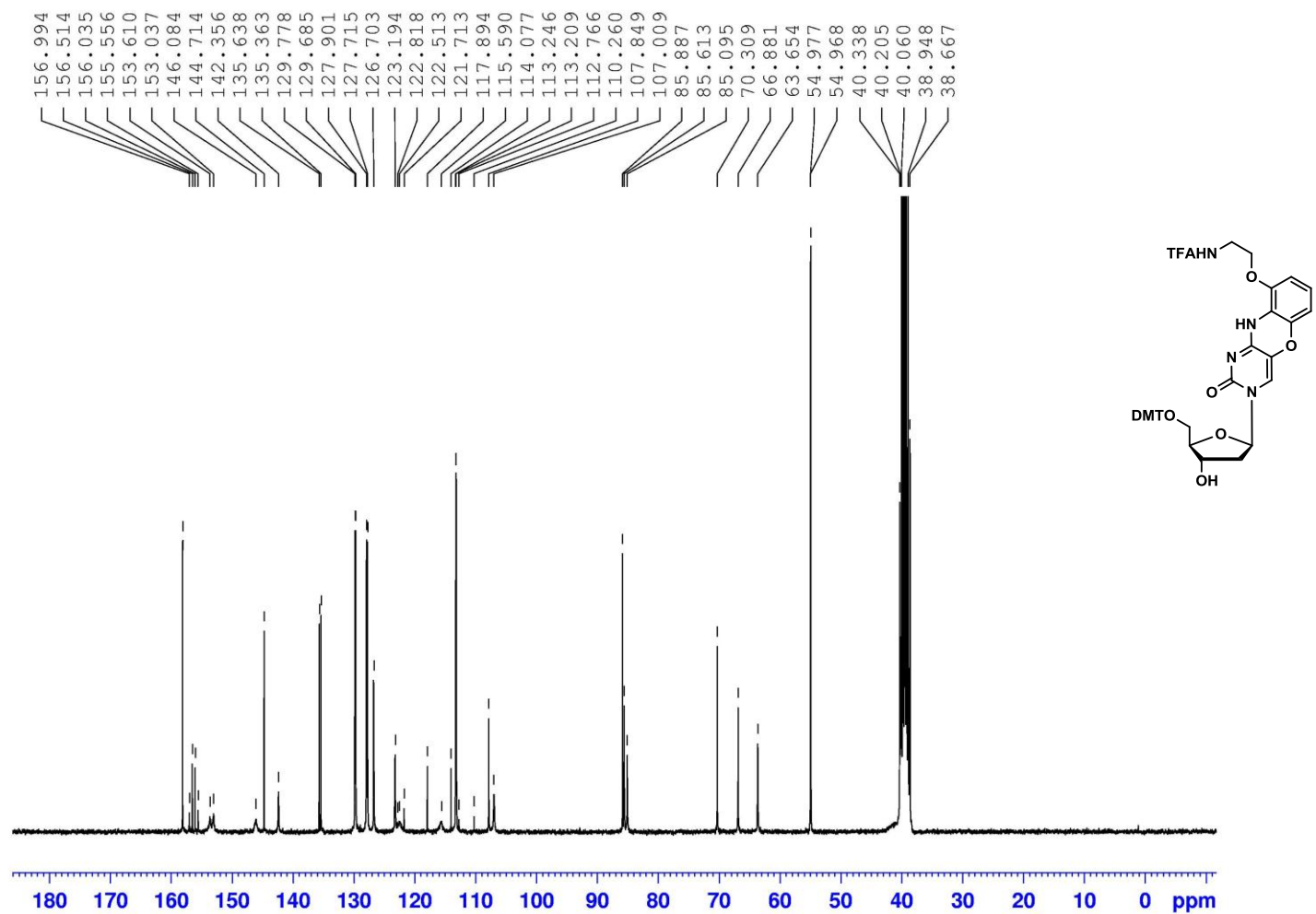


Figure S23.  $^{13}\text{C}$ -NMR spectrum of the DMT-protected G-clamp.

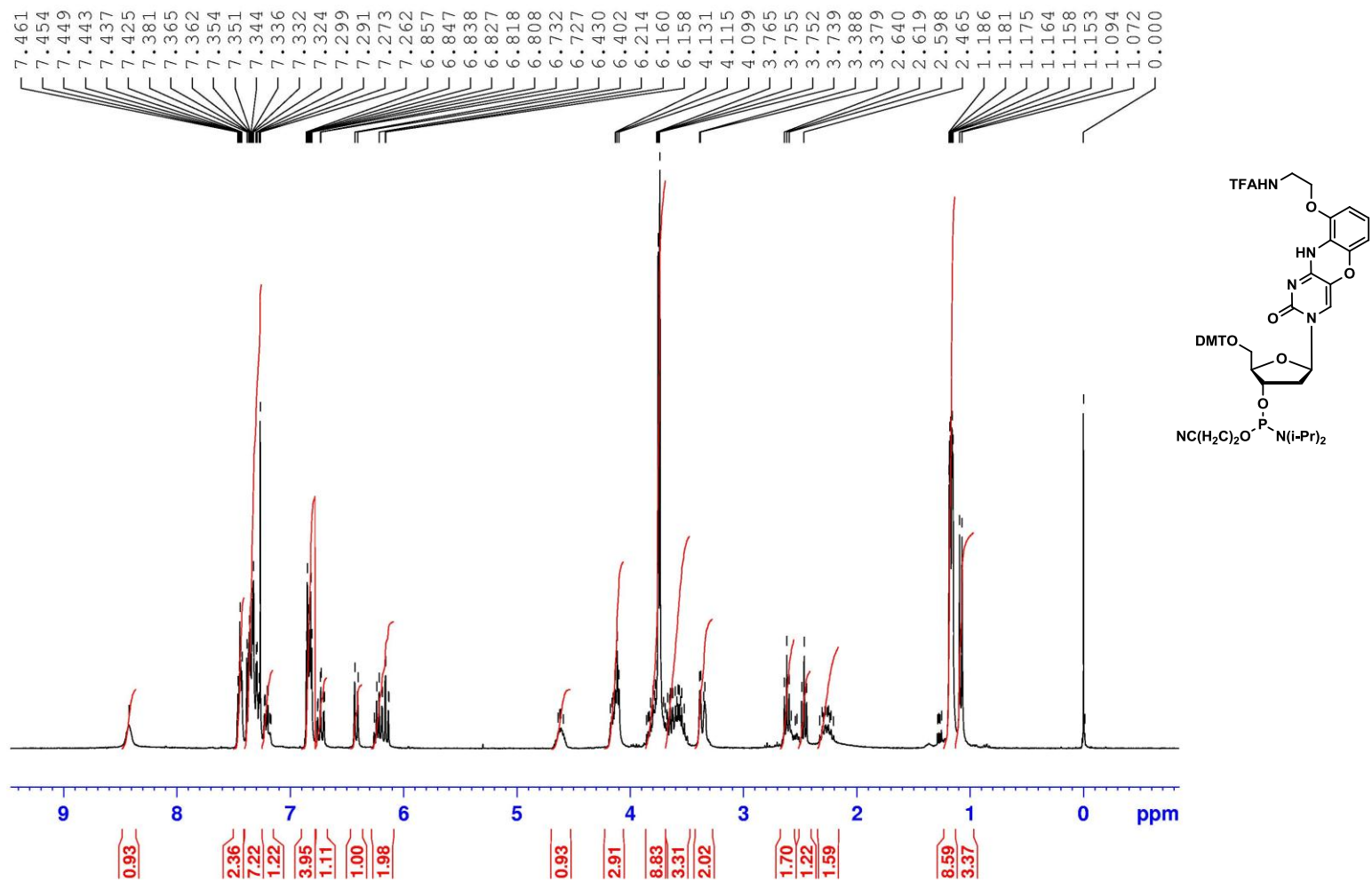


Figure S24. <sup>1</sup>H-NMR spectrum of phosphoramidite 16.

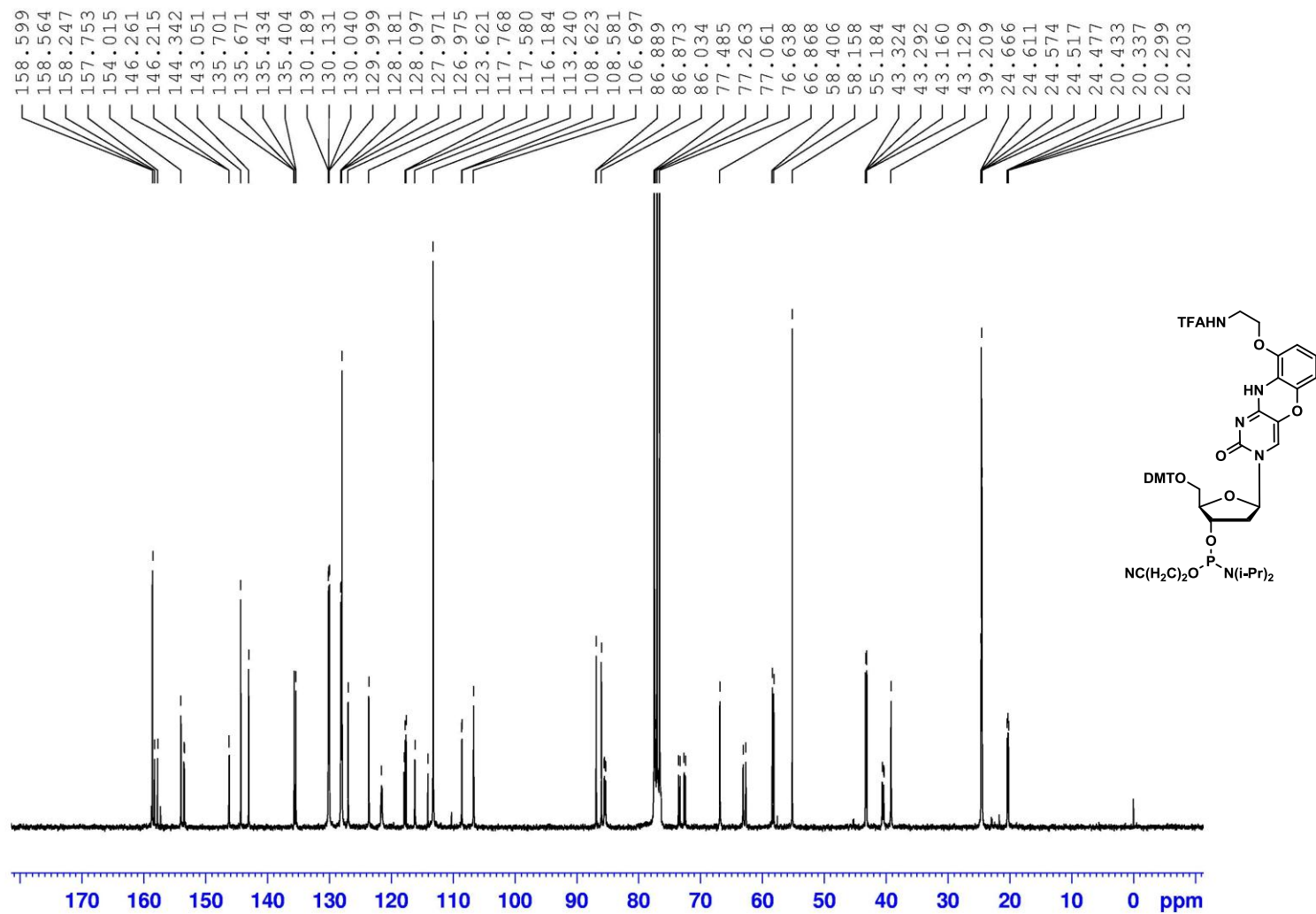
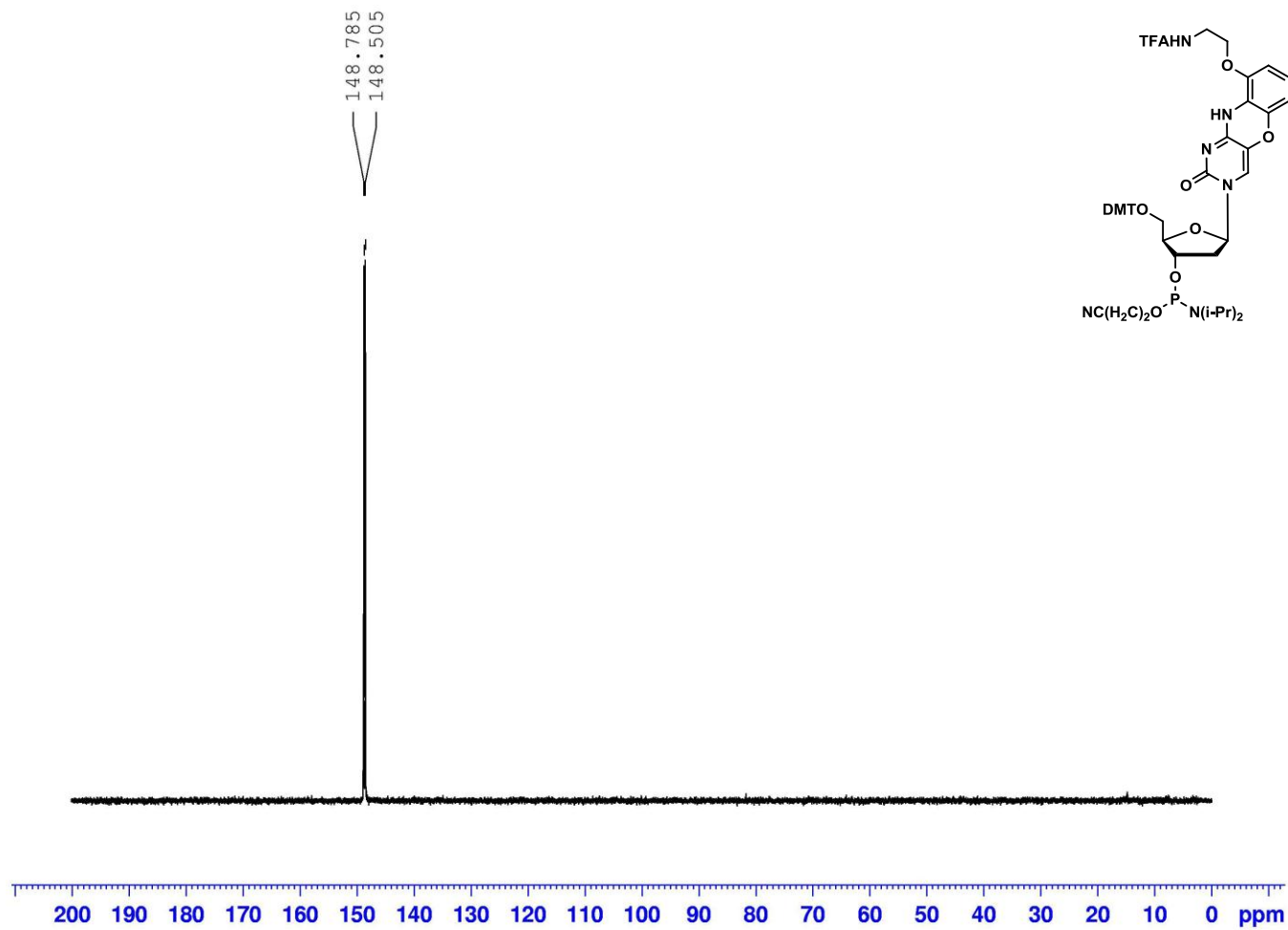


Figure S25. <sup>13</sup>C-NMR spectrum of phosphoramidite **16**.



**Figure S26.**  $^{31}\text{P}$ -NMR spectrum of phosphoramidite **16**.